Foot Placement Compensator Design for Humanoid Walking Based on Discrete Control Lyapunov Function

Chengju Liu, Tong Zhang, Changzhu Zhang, *Member, IEEE*, Ming Liu, and Qijun Chen, *Senior Member, IEEE*

***Abstract*—In this paper, an online foot position compensator (FPC) is proposed for improving the robustness of humanoid walking based on orbital energy conservation and discrete control Lyapunov function (DCLF), with which the asymptotic stability of the humanoid system can be maintained and, thus, the foot placement control is achieved. The online FPC is developed based on linear model predictive control (MPC) by replanning the trajectories of the center of mass (CoM) and properly placing the footsteps to resist external disturbances and recover the walking posture. To further improve the robustness of the humanoid robots to suppress strong external disturbance, a strategy of upper body posture control is proposed. The presented controller stabilizes the humanoid robot by utilizing hip joints to modulate the upper body posture online. Webots simulations and real experiments on a full-body NAO humanoid robot verify the effectiveness of the proposed methods.**

***Index Terms*—Biped walking, discrete control Lyapunov function (DCLF), foot position compensator (FPC), model predictive control (MPC), orbital energy conservation.**

I. Introduction

CURRENTLY, various novel control methods have been proposed to deal with the motion control of robots, such as super-exponential-zeroing neurodynamic approach [1], [2], hybrid multiobjective scheme [3], Jacobian-matrix-adaption method [4], neural network (NN) control [5]–[7], and CPG-inspired control [8]–[11], which have been widely applied to robots. Especially, research in the problem of robust biped walking has become increasingly important and received widespread attention in the recent years [12]–[15]. Robust walking is fundamental for a biped robot to execute tasks in an unstructured environment. In biped walking, the zero moment point (ZMP) is the basic criterion to guarantee the stability [16]–[21]. Biped walking is commonly studied by planning the center of mass (CoM) trajectory such that the ZMP trajectory follows the desired one based on the linear inverted pendulum model (LIPM) or Cart-table model [22]–[27]. The main problem of ZMP-based methods is the discrepancy between the dynamics of the actual robot and the simplified dynamic model which usually causes grate tracking errors or even the instability of the humanoid robots.

To guarantee the adaptive locomotion under external disturbances, such as pushes or uneven walking terrains, a great number of control strategies have been proposed to regulate the CoM or track ZMP reference trajectories through robust feedback schemes [28]–[31]. Hu *et al.* [30] presented a real-time learning framework to improve the robustness of ZMP-based biped walking controllers, using iterative learning control to learn a feedforward compensative ZMP from measured ZMP errors during repetitive locomotion. Mason *et al.* [31] extended simplified walking pattern generators to exploit hand contacts when stability cannot be maintained by stepping. Biological inspired methods, such as central pattern generator methods, are also used to online regulate the CoM or ZMP reference trajectories to improve the adaptability and robustness of biped walking [32]–[38]. In our previous work, an online CoM trajectory modulation method based on CPGs was proposed using sensory feedback to real slope terrain walking [33]. In [34], in order to improve the adaptability, foot trajectory and CoM trajectory generators were proposed to realize uneven terrain adaptive walking. These methods imitate the instantaneous reactive balance strategies of human beings. Castano *et al.* [35] applied a model-based method to compute and predict the next step's position, which allows the robot to restore the nominal and symmetric gait subject to external disturbances. However, there are no physical experiments and upper body posture control in [35].

For strong disturbance rejection during humanoid robot walking, a better way is to apply adjustable foot position strategy to realize online adaptive foot positioning. To reject disturbances for continuous locomotion, Wieber *et al.* [39], Diedam *et al.* [40], and Herdt *et al.* [41] presented a gait pattern generation method with modulating foot position and step duration based on the model predictive control (MPC) scheme.

Manuscript received November 27, 2018; revised February 2, 2019; accepted April 9, 2019. This work was supported in part by the National Natural Science Foundation of China under Grant U1713211, Grant 61673300, and Grant 61573260, and in part by the Basic Research Project of Shanghai Science and Technology Commission under Grant 18DZ1200804, Grant 16JC1401200, and Grant 17511108602. This paper was recommended by Associate Editor S. Nahavandi. *(Corresponding author: Qijun Chen.)*

C. Liu, T. Zhang, C. Zhang, and Q. Chen are with the Department of Electronics and Information Engineering, Tongji University, Shanghai 201804, China (e-mail: liuchengju@tongji.edu.cn; olive_zt@163.com; zhang_changzhu@tongji.edu.cn; qjchen@tongji.edu.cn).

M. Liu is with the Department of Electronic and Computer Engineering, Hong Kong University of Science and Technology, Hong Kong (e-mail: eelium@ust.hk).

Color versions of one or more of the figures in this paper are available online at http://ieeexplore.ieee.org.

Digital Object Identifier 10.1109/TSMC.2019.2912417

Nishiwaki and Kagami [42] developed a control method for biped robust walking by changing the reference ZMP, next step position and duration of the current step. Feng *et al.* [43] presented a step optimization strategy to realize adaptive locomotion in the presence of disturbance by MPC. The control method presented by Kryczka *et al.* [44] not only can regulate the step positions but also can modulate its timing for the robots to recover from the impact of external disturbances. Joe and Oh [14] considered external disturbance as a capture-point error, and a desired ZMP is used to compensate the capture-point error through a capture-point control strategy. In our previous work [45], [46], based on the adjustable nonparametric regression model, we proposed a heteroscedastic sparse GP (HSpGP)-based foot position compensator (FPC) approach to improve the robustness of biped walking. The proposed HSpGP-based FPC approach is nonparametric, which does not need to precisely model the dynamical relationship between the humanoid robot state and the modified walking steps.

In this paper, we focus on improving the robustness and stability of a biped walking under strong external disturbances by compensating the footstep position online. Based on the previous research work, we investigate a strong external disturbance rejection method based on discrete control Lyapunov function (DCLF) and MPC. With the proposed FPC, the trajectories of CoM are replanned, and the foot placement is properly controlled to resist external disturbances and recover the walking position based on Cart-table model. The analytic solutions of foot placements are derived by orbital energy conservation equation and DCLF. The main contributions of this paper are summarized as follows.

1) The dynamics of the humanoid robot are modeled as a cart moving on a massless table, the humanoid robot's leg is considered as a weightless scalable limb of the table, and the kinematic constraints of the robot are not considered. Given the CoM motion equation, the desired CoM and the reference ZMP trajectory can be both generated in real time. The biped walking control can be realized by using inverse kinematics to obtain joint commands from the CoM trajectory.
2) The improvement in humanoid walking performance is evaluated qualitatively by the capacity to recover balance when an external disturbance is applied. Although a proper footstep placement ensures the stability of the robot, it may tip over while walking in an uncertain environment, such as uneven terrain or slopes, as the actual body does not conform to the desired posture due to tracking errors. Therefore, a control strategy is proposed to compensate the upper body posture by utilizing the hip joints to control the inclination of the robot torso online.

The remainder of this paper is organized as follows. Section II presents the MPC. Section III shows the design strategy of the proposed FPC. Section IV develops the upper body posture control method. The presented method is verified in Section V with simulation and real experiments on the humanoid NAO robot. We conclude this paper in Section VI including an outline of our future work.

II. Model Prediction Control

With the MPC algorithms, the optimal and stable trajectory of robot's CoM can be generated based on the dynamic performance of the system to be concerned. As the humanoid robot system is nonlinear, it has been proved that nonlinear MPC method can get better performance and smaller tracking errors than those with linear MPC method. However, the linear MPC method allows shorter computation periods than nonlinear MPC method, therefore, the control loop of the robot system could make a faster response to the change of the environment. Before presenting the linear MPC method, we assume that the humanoid robot is walking on a horizontal plane and thus the robot's CoM is constrained on a horizontal plane, i.e., the height of the CoM is constant. In this case, the movement of the centroid in space is two-dimensional and can be defined as (x, y).

The trajectory of CoM of the humanoid robot is related to the acceleration $\dddot{x}$ and $\dddot{y}$ of the CoM in the constant time period T. Therefore, we can have the humanoid robot's dynamics at discrete-time t_{k+1} as

$$\bar{x}_{k+1} = A\bar{x}_k + B\dddot{x}(t_k) \tag{1}$$

$$\bar{y}_{k+1} = A\bar{y}_k + B\dddot{y}(t_k) \tag{2}$$

where

$$\bar{x}_k = \begin{pmatrix} x(t_k) \\ \dot{x}(t_k) \\ \ddot{x}(t_k) \end{pmatrix},\ \bar{y}_k = \begin{pmatrix} y(t_k) \\ \dot{y}(t_k) \\ \ddot{y}(t_k) \end{pmatrix},\ A = \begin{bmatrix} 1 & T & T^2/2 \\ 0 & 1 & T \\ 0 & 0 & 1 \end{bmatrix}$$

$$B = \begin{bmatrix} T^3/6 \\ T^2/2 \\ T \end{bmatrix}.$$

Let (zmp_k^x, zmp_k^y) be the ZMP position of the humanoid robot

$$zmp_k^x = \begin{bmatrix} 1 & 0 & -Z_c/g \end{bmatrix}\bar{x}_k \tag{3}$$

$$zmp_k^y = \begin{bmatrix} 1 & 0 & -Z_c/g \end{bmatrix}\bar{y}_k \tag{4}$$

where T is the sampling period of the discretized system, Z_c is the height of the humanoid centroid from the ground and supposed to be a constant, and g is the acceleration of gravity.

We can have the relationship between the acceleration, position, and velocity of the CoM and the position of ZMP through (1) recursively

$$X_{k+1} = \begin{bmatrix} x_{k+1} \\ \vdots \\ x_{k+N} \end{bmatrix} = P_{ps}\bar{x}_k + P_{pu}\dddot{X}_k \tag{5}$$

$$\dot{X}_{k+1} = \begin{bmatrix} \dot{x}_{k+1} \\ \vdots \\ \dot{x}_{k+N} \end{bmatrix} = P_{vs}\bar{x}_k + P_{vu}\dddot{X}_k \tag{6}$$

$$\mathrm{ZMP}_{k+1}^x = \begin{bmatrix} zmp_{k+1}^x \\ \vdots \\ zmp_{k+N}^x \end{bmatrix} = P_{zs}\bar{x}_k + P_{zu}\dddot{X}_k \tag{7}$$

where

$$\dddot{X}_k = \begin{bmatrix} \dddot{x}_k \\ \vdots \\ \dddot{x}_{k+N-1} \end{bmatrix} \tag{8}$$

$$P_{ps} = \begin{bmatrix} 1 & T & T^2/2 \\ \vdots & \vdots & \vdots \\ 1 & NT & N^2T^2/2 \end{bmatrix} \tag{9}$$

$$P_{vs} = \begin{bmatrix} 0 & 1 & T \\ \vdots & \vdots & \vdots \\ 0 & 1 & NT \end{bmatrix} \tag{10}$$

$$P_{zs} = \begin{bmatrix} 1 & T & T^2/2 - Z_c/g \\ \vdots & \vdots & \vdots \\ 1 & NT & N^2T^2/2 - Z_c/g \end{bmatrix} \tag{11}$$

$$P_{pu} = \begin{bmatrix} T^3/6 & 0 & 0 \\ \vdots & \ddots & 0 \\ \left(1+3N+3N^2\right)T^3/6 & \cdots & T^3/6 \end{bmatrix} \tag{12}$$

$$P_{vu} = \begin{bmatrix} T^2/2 & 0 & 0 \\ \vdots & \ddots & 0 \\ (1+2N)T^2/2 & \cdots & T^2/2 \end{bmatrix} \tag{13}$$

$$P_{zu} = \begin{bmatrix} T^3/6 - TZ_c/g & 0 & 0 \\ \vdots & \ddots & 0 \\ \left(1+3N+3N^2\right)T^3/6 - TZ_c/g & \cdots & T^3/6 - TZ_c/g \end{bmatrix}. \tag{14}$$

Following the similar line, the relations between Y_{k+1}, $\dot{Y}_{k+1}$, Z^y_{k+1}, $\bar{y}_k$, and $\dddot{Y}_k$ can also be derived.

In MPC, the reference ZMP position trajectory sequence $(\mathrm{ZMP}^{\mathrm{ref}}_{k+1,x}, \mathrm{ZMP}^{\mathrm{ref}}_{k+1,y})$ and the current centroid state are taken as inputs. By adjusting the centroid acceleration and minimizing the objective function, the optimal centroid acceleration can be predicted by tracking the reference ZMP trajectory. The performance of this process can be given by the following quadratic function (QP):

$$\min_{\dddot{X}_k, \dddot{Y}_k} \ \frac{\alpha}{2}\left(\left\|\dddot{X}_k\right\|^2 + \left\|\dddot{Y}_k\right\|^2\right) + \frac{\gamma}{2}\left(\left\|\mathrm{ZMP}_{k+1,x} - \mathrm{ZMP}^{\mathrm{ref}}_{k+1,x}\right\|^2 + \left\|\mathrm{ZMP}_{k+1,y} - \mathrm{ZMP}^{\mathrm{ref}}_{k+1,y}\right\|^2\right). \tag{15}$$

This QP can be re-expressed canonically as

$$\min_{u_k} \ \frac{\alpha}{2} u_k^T Q u_k + p_k^T u_k \tag{16}$$

where

$$u_k = \begin{pmatrix} \dddot{X}_k \\ \dddot{Y}_k \end{pmatrix}, \ Q = \begin{pmatrix} Q' & 0 \\ 0 & Q' \end{pmatrix}, \ Q' = \alpha I + \gamma P_{zu}^T P_{zu}$$

$$p_k = \begin{pmatrix} \gamma P_{zu}^T\left(P_{zu}\bar{x}_k - \mathrm{ZMP}^{\mathrm{ref}}_{k+1,x}\right) \\ \gamma P_{zu}^T\left(P_{zu}\bar{y}_k - \mathrm{ZMP}^{\mathrm{ref}}_{k+1,y}\right) \end{pmatrix}.$$

By minimizing the objective function through QP, we can obtain the optimal u_k, and then the CoM trajectory of the humanoid robot can be planned accordingly.

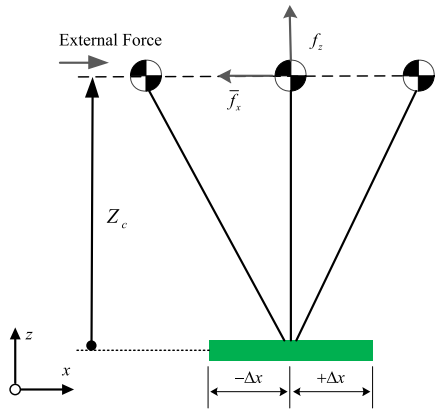

Fig. 1. LIPM.

III. Foot Position Compensator

When a humanoid robot is subjected to disturbances or locomotion on irregular terrains without foot position compensation strategy during the process of walking, the CoM errors become larger than ideal situation, which will lead to an unstable movement. To mimic human's reactions to disturbances during walking, it is natural to change next footstep placement appropriately.

In this paper, we proposed an FPC to adjust the next footstep position of the walking robot. The FPC can modify the contact of the humanoid robot with the walking environment and accordingly replan the reference CoM trajectory such that the humanoid robot can exert a sufficient amount of force to satisfy the novel CoM control requirement. During humanoid walking, the single supporting phase duration is usually much longer than the double supporting phase and the supporting area is much smaller in single supporting phase. Thus, in this paper, the decision of FPC scheme is triggered during the single supporting phase. Since the foot of the robot already contacted with ground cannot be changed, the FPC will come into effect in the next single supporting phase.

As we know, the trajectory planning of a robot can be decomposed into x-direction and y-direction. Hence, the FPC is also set along the x-axis and y-axis, respectively. We only analyze the situation of left leg, thus the result for the right leg is symmetric. Considering the LIPM in Fig. 1, we adopt the LIPM to analyze the FPC by orbital energy conservation method and DCLF. Given the position of the CoM, the dynamics of the system can be written as

$$\ddot{c}_x = g \cdot \frac{c_x}{Z_c} \tag{17}$$

where g denotes the gravitational acceleration and Z_c is the constant height of the CoM.

The solutions of the differential equation (17) are expressed as follows:

$$c_x(t) = c_{x0} \cdot \cosh\left(\frac{t}{T_c}\right) + \dot{c}_{x0} \cdot T_c \sinh\left(\frac{t}{T_c}\right) \tag{18}$$

$$\dot{c}_x(t) = \frac{c_{x0}}{T_c} \cdot \sinh\left(\frac{t}{T_c}\right) + \dot{c}_{x0} \cdot \cosh\left(\frac{t}{T_c}\right) \tag{19}$$

where $T_c = \sqrt{Z_c/g}$, c_{x0} and $\dot{c}_{x0}$ are the initial position and the initial velocity of the CoM with respect to the origin of the LIPM, respectively.

Assuming there are no external disturbances acting on this system, the orbital energy of the LIPM with a fixed pivot can be set as

$$E_{\text{orbital}} = \frac{\dot{c}^2}{2} - \frac{g}{2Z_c}c^2 \tag{20}$$

where $\dot{c}^2/2$, $(g/2Z_c)\cdot c^2$ represent the kinetic energy and potential energy, respectively. Assuming the energy of the system is conserved, (20) allows us to estimate the future CoM states of the robot. In fact, there will always be external disturbances in the system.

When the biped robot moves with a desired periodic gait, the orbital energy expressed in (20) is supposed to be a constant. When subject to external disturbance, the energy of the orbital will be decreased. If the motion velocity wants to be recovered, the orbital energy change need to be compensated and the dissipated energy with respect to the desired energy can be expressed as

$$E_e = E_d - \frac{1}{2}\dot{c}(t_0)^2 - \frac{c(t_0)^2}{2Z_c}g \tag{21}$$

where $E_d = (1/2)\dot{c}_d(t_0)^2 - ([c_d(t_0)^2]/[2Z_c])g$ is the desired orbital energy of the robot.

When $c(t_0) = c_d(t_0)$, (21) can be rewritten as follows:

$$E_e = \frac{1}{2}\Big(\dot{c}(t_0)^2 - \dot{c}_d(t_0)^2\Big). \tag{22}$$

And the required compensated force F_n for the dissipated energy is expressed as

$$\int_{c_0}^{c_f} F_n \delta c = mE_e \tag{23}$$

$$F_n = \frac{mE_e}{2\big(c_f - c(t_0)\big)} \tag{24}$$

where c_f is the final CoM position.

The previous work in [35] applied a model-based method to compute and predict the next step's position, which allows the robot to restore the nominal and symmetric gait subject to external disturbances. In this paper, we investigate a strong external disturbance rejection method based on DCLF and MPC. Fig. 2 depicts the velocity recovery process when the external force is applied to the robot.

Given the desired step length l_s, the period T, and the CoM height Z_c, the initial velocity $\dot{c}_0$ is determined at each step. The CoM velocity $\dot{c}$ is reasonably supposed to be unchanged in each cycle without external disturbance. However, if the robot is subjected to external force, the CoM $\dot{c}$ will change. Therefore, if the velocity of the CoM $\dot{c}$ can be kept constant, the walking of the robot is stable. Moreover, the real velocity $\dot{c}_m$ can be kept close to the desired one at the midstance point through adjusting the foot placement.

The LIPM is used to find the analytic representation of the foot placement, and the orbital energy is constant in one step cycle if there is no external disturbance. And the initial position and end position of the foot with respect to the supporting foot are $c_0 = -l_s/2$ and $c_f = l_s/2$, respectively.

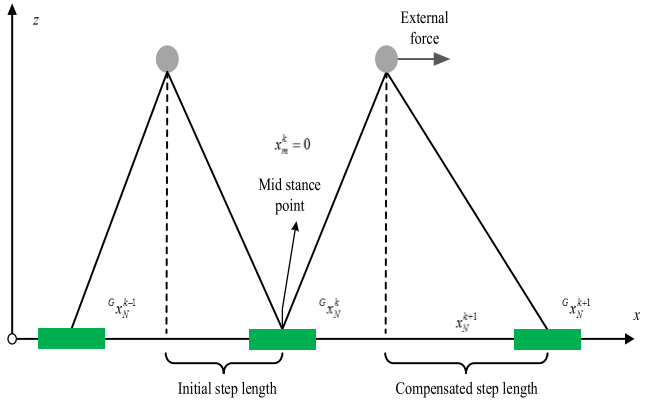

Fig. 2. Velocity recovery process.

When the robot's CoM states changes from one state $(c_1, \dot{c}_1)$ to $(c_2, \dot{c}_2)$, the transition time is

$$\tau = T_c \ln\left[\frac{c_2 + T_c\dot{c}_2}{c_1 + T_c\dot{c}_1}\right]. \tag{25}$$

And we can obtain the following equations, when substituting $(c_1, \dot{c}_1) = (c_0^k, \dot{c}_0^k)$, $(c_2, \dot{c}_2) = (c_f^k, \dot{c}_f^k)$, $c_0^k = -l_s/2$, $c_f^k = l_s/2$, and $\dot{c}_0^k = \dot{c}_f^k$ into (25):

$$T = T_c \ln\left[\frac{\frac{-l_s}{2} + T_c\dot{c}_0^k}{\frac{l_s}{2} + T_c\dot{c}_0^k}\right] \tag{26}$$

$$\dot{c}_0^k = \frac{l_s}{2T_c}\left(\frac{1 + e^{T/T_c}}{1 - e^{T/T_c}}\right). \tag{27}$$

Equation (27) can be rewritten as follows:

$$\dot{c}_0^k = \frac{l_s}{2T_c}\coth\left(\frac{T}{2T_c}\right). \tag{28}$$

Using the orbital energy conservation (20), we have

$$\frac{\dot{c}_1^2}{2} - \frac{g}{2Z_c}c_1^2 = \frac{\dot{c}_2^2}{2} - \frac{g}{2Z_c}c_2^2. \tag{29}$$

Given the velocity $\dot{c}_{\text{now}}$ and the step size of gait cycle, the relationship between the final velocity $\dot{c}_f$ and next foot placement compensation c_N^{k+1} can be obtained as well

$$c_N^{k+1} = \sqrt{\frac{Z_c}{g}\left(\left(\dot{c}_f^k\right)^2 - \dot{c}_{\text{now}}^2\right) + \left(c_N^k\right)^2}. \tag{30}$$

To guarantee the asymptotic stability of the system, we introduce the DCLF [47] to obtain the next foot placement compensation c_N^{k+1}. First, we define the Lyapunov function as

$$V(\Delta\dot{c}_k) = \Delta\dot{c}_k^2 = (\dot{c}_k - \dot{c}_{\text{ideal}})^2 \tag{31}$$

where $\Delta\dot{c}_k$ represents the error of CoM velocity between CoM velocity $\dot{c}_k$ and ideal CoM velocity $\dot{c}_{\text{ideal}}$.

From (31), we know that $V(\Delta\dot{c}_k) \geq 0$. According to the Lyapunov stability theory, if the system is asymptotically stable, then the derivative of Lyapunov function should satisfy the following condition:

$$\dot{V}(\Delta\dot{c}_k) < 0. \tag{32}$$

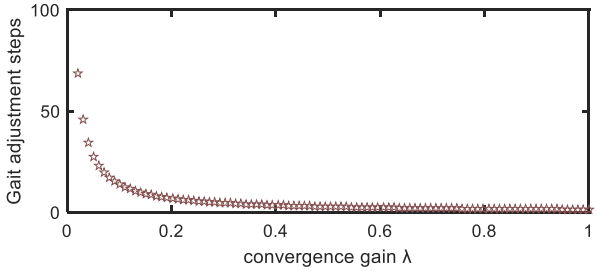

Fig. 3. Influence of convergence coefficient λ on gait adjustment.

Because the humanoid robot system is a discrete system, we can get the following relationship:

$$\begin{aligned}\dot{V}(\Delta\dot{c}_k) &= V(\Delta\dot{c}_{k+1}) - V(\Delta\dot{c}_k)\\ &= (\dot{c}_{k+1} - \dot{c}_{\text{ideal}})^2 - (\dot{c}_k - \dot{c}_{\text{ideal}})^2. \end{aligned} \tag{33}$$

In order to achieve the asymptotic stability of the robot system through discrete control, it is required that the following inequality (34) holds such that the closed-loop system can be exponentially stable:

$$\dot{V}(\Delta\dot{c}_k) = V(\Delta\dot{c}_{k+1}) - V(\Delta\dot{c}_k) = -\lambda V(\Delta\dot{c}_k) < 0, \quad 0 < \lambda < 1 \tag{34}$$

where λ is the exponential convergence coefficient belonging to [0, 1].

Then according to (33) and (34), we have the following equation:

$$\dot{c}_{k+1} = \dot{c}_{\text{ideal}} + \sqrt{(1-\lambda)(\dot{c}_k - \dot{c}_{\text{ideal}})^2}. \tag{35}$$

Letting $\dot{c}_f^k = \dot{c}_{k+1}$, $\dot{c}_{\text{now}} = \dot{c}_k$, and substituting (35) into (30), we can get the step compensation

$$c_N^{k+1} = \sqrt{\frac{Z_c}{g}\left(\left(\dot{c}_{\text{ideal}} + \sqrt{(1-\lambda)(\dot{c}_k - \dot{c}_{\text{ideal}})^2}\right)^2 - \dot{c}_k^2\right) + \left(c_N^k\right)^2}. \tag{36}$$

Hence, given the index convergence coefficient λ, ideal CoM velocity $\dot{c}_{\text{ideal}}$, real CoM velocity $\dot{c}_k$, and the step size in the current gait cycle c_N^k, we can calculate the next foot placement in the x-axis by using (36). Next foot placement in y-axis can also be obtained by following the similar idea. In addition, a single foot supporting phase executes only once calculating process to guarantee the calculation speed. With the proposed control, the stability of the closed-loop system is achieved via the Lyapunov's stability theory.

Fig. 3 shows the effect of the convergence factor λ on the gait adjustment steps, from which it can be seen that the convergence coefficient and the gait adjustment steps required for convergence can be approximated logarithmically. As the value of the convergence coefficient increases, the number of gait adjustment steps required for convergence decreases.

When $\lambda < 0.2$, the robot's gait needs to be adjusted by more than ten steps in order to be able to converge. However, we require the humanoid robot to quickly stabilize against the external disturbance in practical applications. Therefore, the value of the convergence coefficient in this range is not applicable. In an ideal situation, when the humanoid robot is disturbed, the speed of rebalance is required to be as fast as possible. However, the faster the convergence is, the more pressure the robot joint receives. At one extreme, it may cause damage to the robot joints and even affect the balance of the robot. Therefore, the values of the convergence coefficients are usually set to belong the interval of [0.4, 0.6].

IV. Upper Body Posture Control

The overall architecture of the control strategy is shown in Fig. 4. A posture control method presented to adjust the body angles with the hip joints to improve the walking stability.

For the upper body posture control, the adjusting angles of hip joints ($\Delta\theta_{\text{HipPitch}}$, $\Delta\theta_{\text{HipRoll}}$) by applying a PD controller can be expressed as

$$\Delta\theta_{\text{HipPitch}} = K_{p1}\left(\theta_p - \hat{\theta}_p\right) + K_{d1}\left(\dot{\theta}_p - \dot{\hat{\theta}}_p\right) \tag{37}$$

$$\Delta\theta_{\text{HipRoll}} = K_{p2}\left(\theta_r - \hat{\theta}_r\right) + K_{d2}\left(\dot{\theta}_r - \dot{\hat{\theta}}_r\right) \tag{38}$$

where K_p and K_d are the proportional gain and differential gain, respectively, (θ_p, θ_r) are the desired body angles in x-axis and y-axis, and $(\dot{\theta}_p, \dot{\theta}_r)$ are the desired body angular velocities. $(\hat{\theta}_p, \hat{\theta}_r)$ are the measured body angles and $(\dot{\hat{\theta}}_p, \dot{\hat{\theta}}_r)$ are the measured body angular velocities. This control method is executed at every moment of the locomotion process.

V. Simulation and Real Experiments

Simulations and real robot experiments are setup using the humanoid NAO platform [Fig. 5(a)]. NAO has 26 degrees of freedom. Each leg weighs nearly as much as the body, and the links are made of plastic. This makes the dynamics of the robot substantially different from the simplified Cart-table model. Furthermore, the deformation of plastic links can be caused by the disturbance. Simulations are conducted using the Webots simulation platform as shown in Fig. 5(b).

The body attitude θ can be estimated using the gyroscope and accelerometer of the NAO robot. A high-pass filter (HF) and a low-pass filter (LF) are used to further obtain the dynamic and static characteristics of θ_{acc} and θ_{gyro}, respectively. The calculation method designed for this paper is shown in Figs. 6 and 7, where θ_{acc} is the body attitude calculated by the accelerometer, and θ_{gyro} is the body attitude measured by the gyroscope. The calculation equation is expressed as

$$\theta = \text{GainL} \cdot \text{LF}(\theta_{\text{acc}}) + \text{GainH} \cdot \text{HF}\left(\theta_{\text{gyro}}\right). \tag{39}$$

A. Robust Biped Walking Under Unknown Interference

First, NAO robot is walking straight forward on a flat terrain without disturbances with a walking step size of 0.1 m. The parameters of the PD controller are set as $K_p = 1.4$, $K_d = 0.5$, and the convergence coefficient set as $\lambda = 0.45$ in the following experiments. In this case, NAO is pushed to its forward (x-axis direction) while on left single foot supporting phase. NAO takes several steps to recover the locomotion. A force of about 10.084 N is applied to the centroid of NAO, and the force duration is approximately 0.6 s. Fig. 8 shows

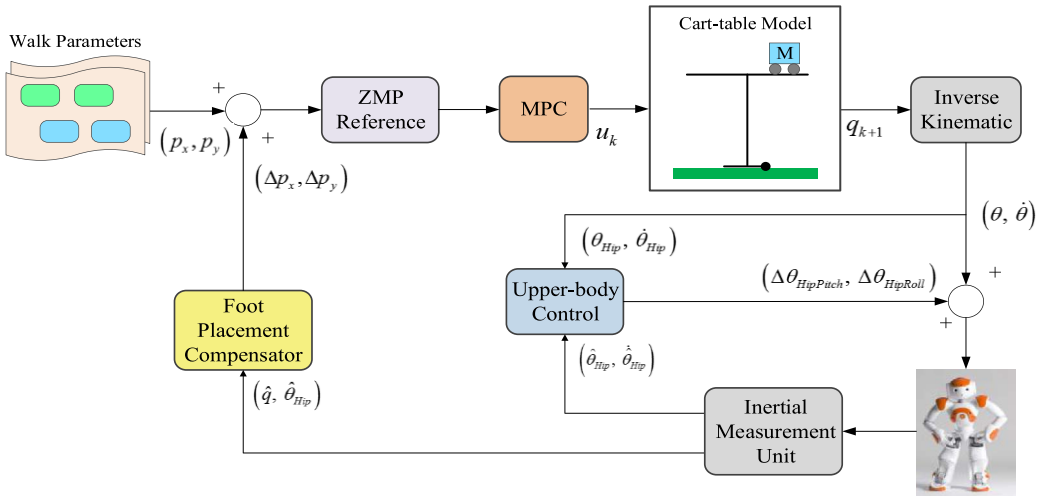

Fig. 4. Diagram of the walking control with an FPC.

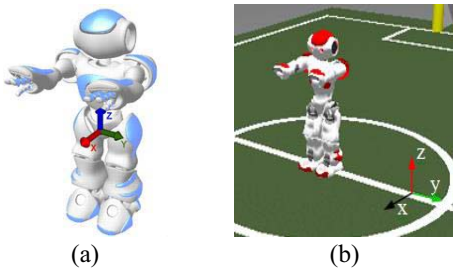

Fig. 5. Robot platform. (a) NAO robot. (b) ODE-based simulation environment.

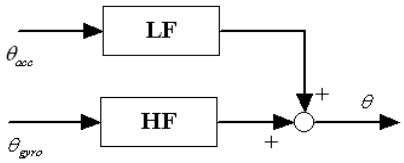

Fig. 6. Calculation of the body attitude angle.

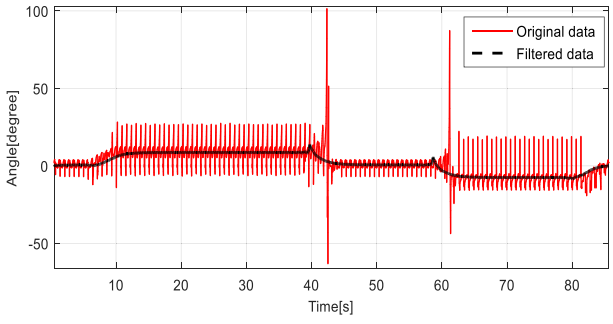

Fig. 7. θ_{pitch} before and after filtering.

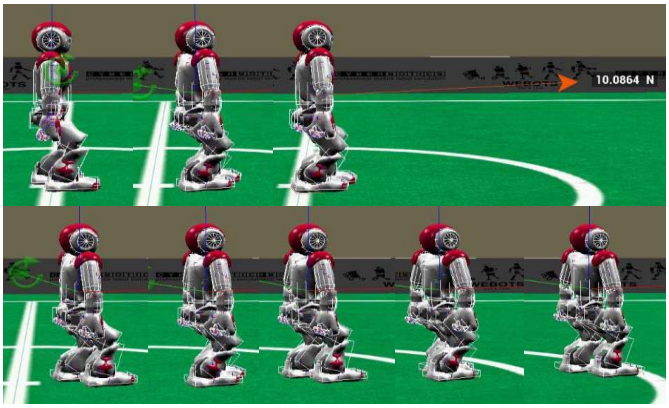

Fig. 8. Snapshot sequences of NAO recovering from disturbance push.

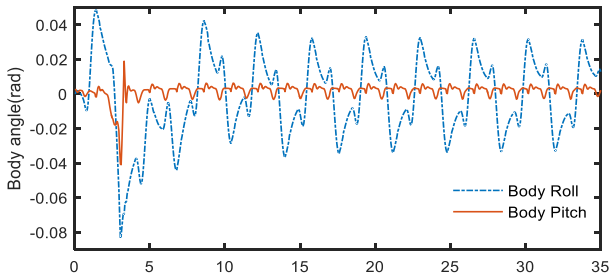

Fig. 9. Measured upper body attitude.

the snapshots of this experiment. From the experiment snapshots, we can figure out that when the external force is applied, it increases the next foot placement to resist the external disturbance.

The body attitude during robust walking is shown in Fig. 9. The body roll curve reaches a peak at approximately 3.5 s, which decrease to -0.085 rad. The foot placements in the experiment of the robot are shown in Fig. 10, and the maximum foot placement along the x-axis is 0.062 at about the fourth step.

Fig. 11 compares the reference ZMP and real ZMP. About 3 s, the real ZMP is fluctuating but with the effect of FPC the real ZMP not being out of the support polygon. Due to the delays or errors in sensors, there are some difference between the actual ZMP and the ideal trajectories.

For the first real robot experiment, the robot is normally walking but pushed from the front with a force Gauge. Without

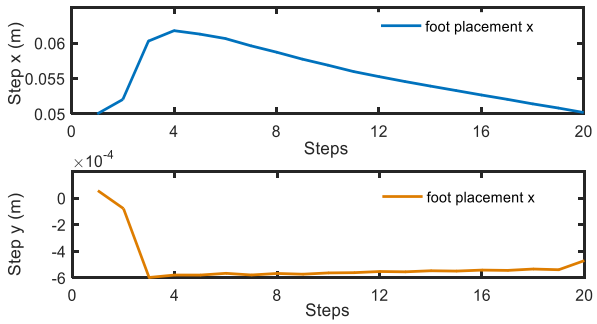

Fig. 10. Foot placements.

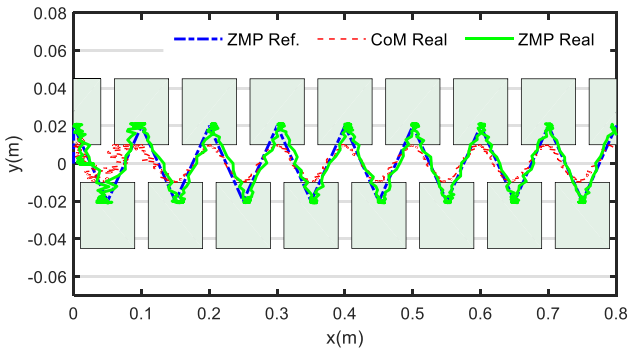

Fig. 11. ZMP trajectories.

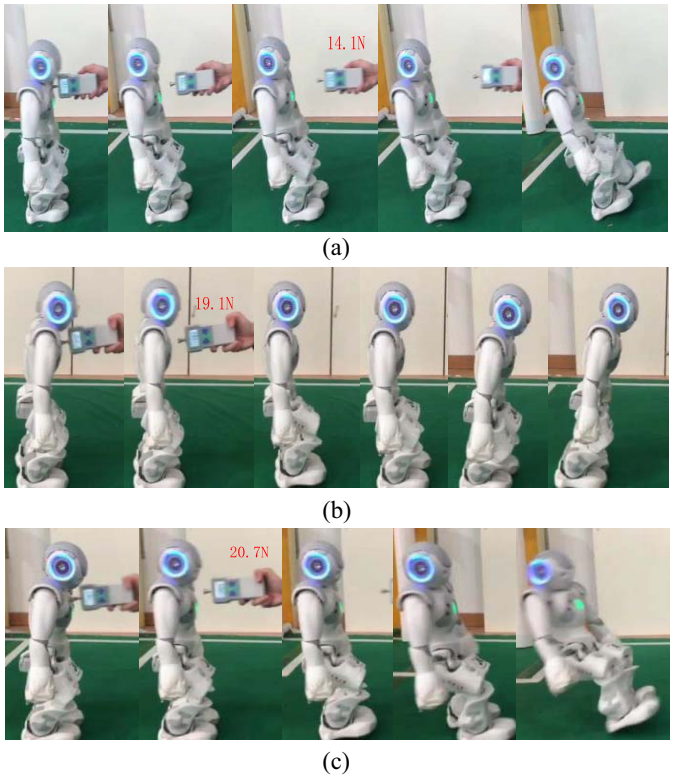

Fig. 12. Snapshot sequences of a real robot recovering from a push. (a) Snapshot sequences of a real robot walking without FPC. (b) Snapshot sequences of a real robot walking with FPC. (c) Snapshot sequences of the NAO Robot's maximum interference tolerance experiment.

the proposed FPC, the robot falls down quickly when suffering from external push (about 14.1 N). But with the FPC, when subjected to 19.1 N thrust, the robot increases the size

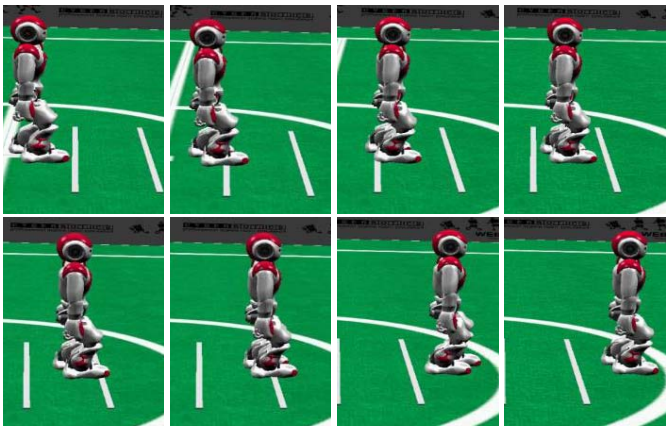

Fig. 13. Snapshot sequences of locomotion on uneven terrain.

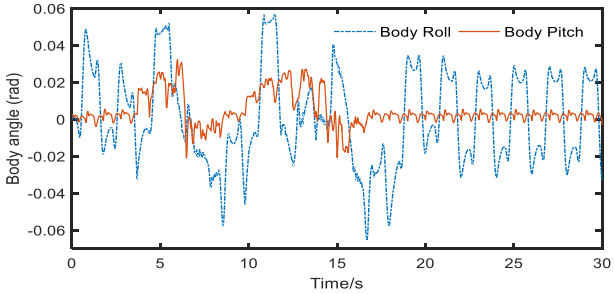

Fig. 14. Measured upper body attitude.

of its foot placements in the following several steps and retains balance eventually. The snapshots of the experiment in side view are shown in Fig. 12(a) and (b). Fig. 12(c) shows the snapshots of the experiment of NAO Robot's maximum tolerance to interference.

With the proposed FPC in this paper, when the thrust is more than 19 N, the robot can still maintain balance by adjusting its foot placement. The maximum thrust is approximately 20.5 N. In the method proposed in [36], the robot can only suffer a momentum impact of 1.13 N. Compared with the previous work of [37], [45], and [46], humanoid Robot's maximum interference tolerance has been greatly improved. The comparative experiments demonstrate that the presented FPC is valid and enhances the robustness of the humanoid robots considerably.

B. Walking on Uneven Terrain

The motion performance over the uneven walking terrain is verified in the second experiment. The NAO robot walks forward with step size of 0.1 m and there are two white obstacles on the robot's moving path. The size of the two obstacles are both 0.8 m × 0.02 m × 0.01 m. Fig. 13 shows the snapshots of the real experiment.

Fig. 14 shows the measured attitude of the upper body using sensor fusion. Due to the uneven terrain, the pitch angle increases at about 4 s and 8 s, the maximum is 0.03 rad at about 6.5 s. The roll angle decreases at 7 s and 17 s.

Fig. 15 depicts the foot placement from the start to the end of the walking. The foot placement along the x-axis decreases

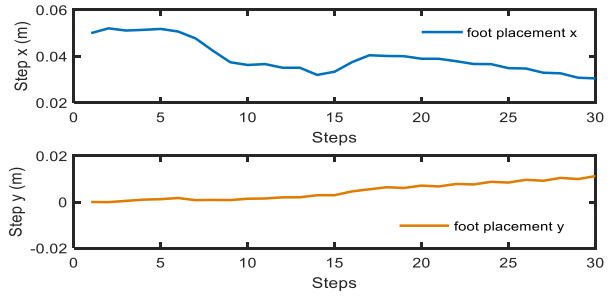

Fig. 15. Foot placements.

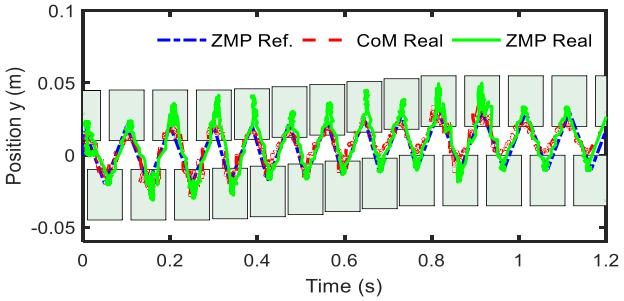

Fig. 16. ZMP trajectories.

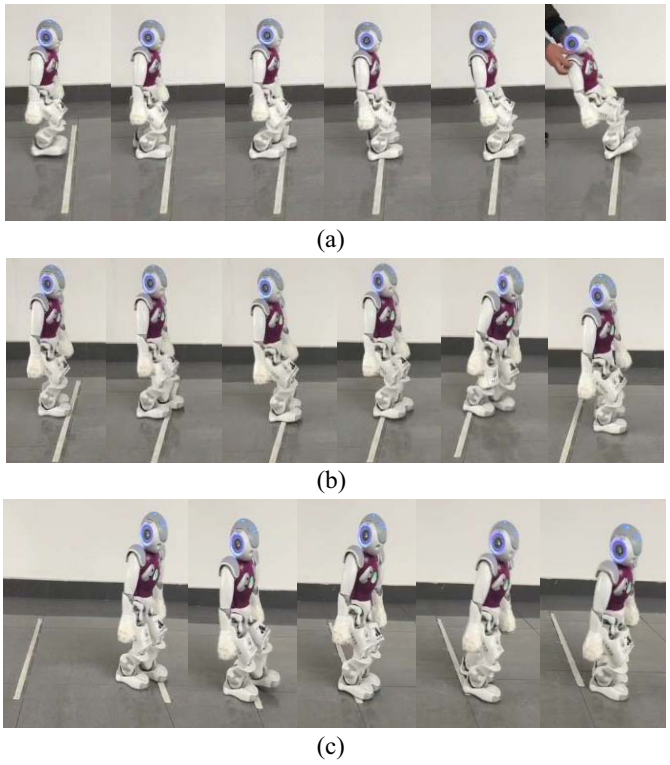

Fig. 17. Snapshot sequences of a real robot experiment walking on uneven terrain. (a) Snapshots of walking without FPC. (b) Snapshots of walking with FPC.

from the fifth step, and the minimum x-axis foot placement is 0.032 m at the 14th step. The foot placement along the y-axis increases during the walking process. Fig. 16 illustrates the reference and actual ZMP trajectories throughout the walking process.

Fig. 17 shows the snapshots of side-view real robot experiments. There are two white obstacles on robot's walking path with size both given by 0.8 m $\times$ 0.02 m $\times$ 0.01 m. Without FPC, when the humanoid robot crosses the first obstacle, the posture of the body changes drastically due to the change of the contact area of the foot and thus the robot falls backward. But with the action of FPC, when the robot's posture changes, it makes several continuous larger steps to reduce the disturbances and successfully walks through the obstacles.

VI. Conclusion

This paper proposed an online FPC for biped robust walking based on orbital energy conservation and DCLF. The presented control algorithm can generate proper foot placement and does not require complex calculations though this method can only withstand limited external disturbance. A posture control method is added to further improve the robots' ability to resist external strong perturbations. Some simulation and experimental results verify the proposed strategy can realize biped robust walking under strong external pushes or walk through uneven terrain.

However, it should be noted that the online parameters learning is not considered in this paper, as an extension, the nonparametric regression model, such as Gaussian process model, which does not require precise modeling of the dynamic relationship between the humanoid robot state and the modified footsteps, will be considered to locally update the parameters of the control system in real-time in the future work.

Furthermore, in order to evaluate the rebalance performance of the novel method, survival rate index will be developed to compare with the current work. The survival rate will defined as follows: given a certain number of steps in a complete walk and a certain number of trials, the survival rate is the number of successful completion of walking without falling. The proposed survival rate index will provide a statistical evaluation of robot walking performance.

References

[1] D. Chen, S. Li, and Q. Wu, "Rejecting chaotic disturbances using a super-exponential-zeroing neurodynamic approach for synchronization of chaotic sensor systems," *Sensors*, vol. 19, no. 1, 2019, Art. no. E74.

[2] D. Chen and Y. Zhang, "Robust zeroing neural-dynamics and its time-varying disturbances suppression model applied to mobile robot manipulators," *IEEE Trans. Neural Netw. Learn. Syst.*, vol. 29, no. 9, pp. 4385–4397. Sep. 2018.

[3] D. Chen and Y. Zhang, "A hybrid multi-objective scheme applied to redundant robot manipulators," *IEEE Trans. Autom. Sci. Eng.*, vol. 14, no. 3, pp. 1337–1350, Jul. 2017.

[4] D. Chen, Y. Zhang, and S. Li, "Tracking control of robot manipulators with unknown models: A Jacobian-matrix-adaption method," *IEEE Trans. Ind. Informat.*, vol. 14, no. 7, pp. 3044–3053, Jul. 2018.

[5] W. He, Z. Li, and C. L. P. Chen, "A survey of human-centered intelligent robots: Issues and challenges," *IEEE/CAA J. Automatica Sinica*, vol. 4, no. 4, pp. 602–609, Oct. 2017.

[6] W. He and Y. Dong, "Adaptive fuzzy neural network control for a constrained robot using impedance learning," *IEEE Trans. Neural Netw. Learn. Syst.*, vol. 29, no. 4, pp. 1174–1186, Apr. 2018.

[7] C.-F. Juang and Y.-T. Yeh, "Multiobjective evolution of biped robot gaits using advanced continuous ant-colony optimized recurrent neural networks," *IEEE Trans. Cybern.*, vol. 48, no. 6, pp. 1910–1922, Jun. 2018.

[8] F. Dzeladini, N. Ait-Bouziad, and A. Ijspeert, "CPG-based control of humanoid robot locomotion," in *Humanoid Robotics: A Reference*. Dordrecht, The Netherlands: Springer, 2018, pp. 1–35.
[9] A. J. Ijspeert, "Central pattern generators for locomotion control in animals and robots: A review," *Neural Netw.*, vol. 21, no. 4, pp. 642–653, 2008.
[10] Q. Wu, C. Liu, J. Zhang, and Q. Chen, "Survey of locomotion control of legged robots inspired by biological concept," *Sci. China F Inf. Sci.*, vol. 52, no. 10, pp. 1715–1729, 2009.
[11] J. Yu, M. Tan, J. Chen, and J. Zhang, "A survey on CPG-inspired control models and system implementation," *IEEE Trans. Neural Netw. Learn. Syst.*, vol. 25, no. 3, pp. 441–456, Mar. 2014.
[12] H. Jeong, I. Lee, O. Sim, K. Lee, and J.-H. Oh, "A robust walking controller optimizing step position and step time that exploit advantages of footed robot," *Robot Auton. Syst.*, vol. 113, pp. 10–22, Mar. 2019.
[13] K. A. Hamed and R. D. Gregg, "Decentralized event-based controllers for robust stabilization of hybrid periodic orbits: Application to underactuated 3D bipedal walking," *IEEE Trans. Autom. Control*, to be published.
[14] H.-M. Joe and J.-H. Oh, "Balance recovery through model predictive control based on capture point dynamics for biped walking robot," *Robot Auton. Syst.*, vol. 105, pp. 1–10, Jul. 2018.
[15] Z. Yu *et al.*, "Disturbance rejection for biped walking using zero-moment point variation based on body acceleration," *IEEE Trans. Ind. Informat.*, vol. 15, no. 4, pp. 2265–2276, Apr. 2019.
[16] M. Vukobratović and B. Borovac, "Zero-moment point—Thirty five years of its life," *Int. J. Humanoid Robot*, vol. 1, no. 1, pp. 157–173, 2004.
[17] H.-K. Shin and B. K. Kim, "Energy-efficient gait planning and control for biped robots utilizing vertical body motion and allowable ZMP region," *IEEE Trans. Ind. Electron.*, vol. 62, no. 4, pp. 2277–2286, Apr. 2015.
[18] Q. Huang *et al.*, "Planning walking patterns for a biped robot," *IEEE Trans. Robot. Autom.*, vol. 17, no. 3, pp. 280–289, Jun. 2001.
[19] S. Park and J. Oh, "Real-time continuous ZMP pattern generation of a humanoid robot using an analytic method based on capture point," *Adv. Robot.*, vol. 33, no. 1, pp. 33–48, 2019.
[20] T. H. Luat and Y.-T. Kim, "Fuzzy control for walking balance of the biped robot using ZMP criterion," *Int. J. Humanoid Robot.*, vol. 14, no. 2, pp. 1–12, 2017.
[21] S. Kim, K. Hirota, T. Nozaki, and T. Murakami, "Human motion analysis and its application to walking stabilization with COG and ZMP," *IEEE Trans. Ind. Informat.*, vol. 14, no. 11, pp. 5178–5186, Nov. 2018.
[22] S. Kajita *et al.*, "Biped walking stabilization based on linear inverted pendulum tracking," in *Proc. IEEE/RSJ Int. Conf. Intell. Robots Syst.*, Taipei, Taiwan, 2010, pp. 4489–4496.
[23] S. Kajita, "Linear inverted pendulum-based gait," *Humanoid Robotics: A Reference*. Dordrecht, The Netherlands: Springer, 2019, pp. 905–922.
[24] C. Liu, J. Ning, and Q. Chen, "Dynamic walking control of humanoid robots combining linear inverted pendulum mode with parameter optimization," *Int. J. Adv. Robot. Syst.*, vol. 15, no. 1, pp. 1–15, 2018.
[25] T.-H. S. Li, Y.-F. Ho, P.-H. Kuo, Y.-T. Ye, and L.-F. Wu, "Natural walking reference generation based on double-link LIPM gait planning algorithm," *IEEE Access*, vol. 5, pp. 2459–2469, 2017.
[26] J.-W. Luo, Y.-L. Fu, and S.-G. Wang, "3D stable biped walking control and implementation on real robot," *Adv. Robot*, vol. 31, no. 12, pp. 634–649, 2017.
[27] J.-W. Heo and J.-H. Oh, "Biped walking pattern generation using an analytic method for a unit step with a stationary time interval between steps," *IEEE Trans. Ind. Electron.*, vol. 62, no. 2, pp. 1091–1100, Feb. 2015.
[28] M. Kim and S. H. Collins, "Once-per-step control of ankle push-off work improves balance in a three-dimensional simulation of bipedal walking," *IEEE Trans. Robot.*, vol. 33, no. 2, pp. 406–418, Apr. 2017.
[29] Z. Yu *et al.*, "Gait planning of omnidirectional walk on inclined ground for biped robots," *IEEE Trans. Syst., Man, Cybern., Syst.*, vol. 46, no. 7, pp. 888–897, Jul. 2016.
[30] K. Hu, C. Ott, and D. Lee, "Learning and generalization of compensative zero-moment point trajectory for biped walking," *IEEE Trans. Robot.*, vol. 32, no. 3, pp. 717–725, Jun. 2016.
[31] S. Mason, N. Rotella, S. Schaal, and L. Righetti, "An MPC walking framework with external contact forces," in *Proc. IEEE Int. Conf. Robot. Autom.*, Brisbane, QLD, Australia, 2018, pp. 1785–1790.
[32] X. Chen *et al.*, "Bioinspired control of walking with toe-off, heel-strike, and disturbance rejection for a biped robot," *IEEE Trans. Ind. Electron.*, vol. 64, no. 10, pp. 7962–7971, Oct. 2017.
[33] C. J. Liu, D. W. Wang, and Q. J. Chen, "Central pattern generator inspired control for adaptive walking of biped robots," *IEEE Trans. Syst., Man, Cybern., Syst.*, vol. 43, no. 5, pp. 1206–1215, Sep. 2013.
[34] C. J. Liu, D. W. Wang, E. D. Goodman, and Q. Chen, "Adaptive walking control of biped robots using online trajectory generation method based on neural oscillators," *J. Bionic Eng.*, vol. 13, no. 4, pp. 572–584, 2016.
[35] J. A. Castano, Z. Li, C. Zhou, N. Tsagarakis, and D. Caldwell, "Dynamic and reactive walking for humanoid robots based on foot placement control," *Int. J. Humanoid Robot*, vol. 13, no. 2, 2016, Art. no. 1550041.
[36] O. Urbann and M. Hofmann, "A reactive stepping algorithm based on preview controller with observer for biped robots," in *Proc. IEEE/RSJ Int. Conf. Intell. Robot. Syst.*, Daejeon, South Korea, Oct. 2016, pp. 5324–5331.
[37] A. A. Saputra, J. Botzheim, I. A. Sulistijono, and N. Kubota, "Biologically inspired control system for 3-D locomotion of a humanoid biped robot," *IEEE Trans. Syst., Man, Cybern., Syst.*, vol. 4, no. 7, pp. 898–911, Jul. 2016.
[38] Y. Wang, X. Xue, and B. Chen, "Matsuoka's CPG with desired rhythmic signals for adaptive walking of humanoid robots," *IEEE Trans. Cybern.*, to be published. doi: 10.1109/TCYB.2018.2870145.
[39] P.-B. Wieber, "Trajectory free linear model predictive control for stable walking in the presence of strong perturbations," in *Proc. IEEE-RAS Int. Conf. Humanoid Robots*, Genoa, Italy, 2006, pp. 137–142.
[40] H. Diedam, D. Dimitrov, P.-B. Wieber, K. Mombaur, and M. Diehl, "Online walking gait generation with adaptive foot positioning through linear model predictive control," in *Proc. IEEE/RSJ Int. Conf. Intell. Robots Syst.*, Nice, France, 2008, pp. 1121–1126.
[41] A. Herdt *et al.*, "Online walking motion generation with automatic footstep placement," *Adv. Robot.*, vol. 24, nos. 5–6, pp. 719–737, 2010.
[42] K. Nishiwaki and S. Kagami, "Strategies for adjusting the ZMP reference trajectory for maintaining balance in humanoid walking," in *Proc. IEEE Int. Conf. Robot. Autom.*, Anchorage, AK, USA, 2010, pp. 4230–4246.
[43] S. Feng, X. Xinjilefu, C. G. Atkeson, and J. Kim, "Robust dynamic walking using online foot step optimization," in *Proc. IEEE/RSJ Int. Conf. Intell. Robots Syst.*, Daejeon, South Korea, 2016, pp. 5373–5378.
[44] P. Kryczka, P. Kormushev, N. G. Tsagarakis, and D. G. Caldwell, "Online regeneration of bipedal walking gait pattern optimizing footstep placement and timing," in *Proc. IEEE/RSJ Int. Conf. Intell. Robots Syst.*, Hamburg, Germany, 2015, pp. 3352–3357.
[45] T. Xu, Q. Chen, and Z. Cai, "Rebalance strategies for humanoids walking by foot positioning compensator based on adaptive heteroscedastic SpGPs," in *Proc. IEEE Int. Conf. Robot. Autom.*, Shanghai, China, 2011, pp. 563–568.
[46] C. Liu, T. Xu, D. Wang, and Q. Chen, "Active balance of humanoids with foot positioning compensation and non-parametric adaptation," *Robot Auton. Syst.*, vol. 75, pp. 297–309, Jan. 2016.
[47] P. A. Bhounsule and A. Zamani, "A discrete control Lyapunov function for exponential orbital stabilization of the simplest walker," *J. Mech. Robot.*, vol. 9, no. 5, p. 8, 2017.

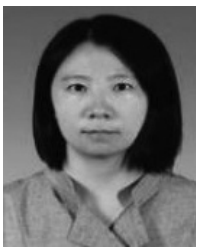

Chengju Liu received the Ph.D. degree in control theory and control engineering from Tongji University, Shanghai, China, in 2011.

From 2011 to 2012, she was with the BEACON Center, Michigan State University, East Lansing, MI, USA, as a Research Associate. From 2011 to 2013, she was a Post-Doctoral Researcher with Tongji University, where she is currently a Professor with the College of Electrical and Information Engineering. Her current research interests include intelligent control, motion control of legged robots, and evolutionary computation.

Tong Zhang received the graduation degree in control theory and control engineering from Tongji University, Shanghai, China, in 2018, where he is currently pursuing the master's degree in control theory and control engineering.

His current research interest includes locomotion of biped robot.

Changzhu Zhang (M'11) received the B.S. degree in automation from Qufu Normal University, Rizhao, China, in 2007, the M.S. degree in control science and engineering from the Harbin Institute of Technology, Harbin, China, in 2009, and the Ph.D. degree in mechatronics engineering from the City University of Hong Kong, Hong Kong, in 2012.

From 2013 to 2014, he was with the Institute of Advanced Study, Tongji University, Shanghai, China, as an Associate Professor. Since 2017, he has been a Research Fellow with the Department of Informatics, King's College London, London, U.K. Since 2014, he has been with the College of Electrical and Information Engineering, Tongji University, where he is currently an Associate Professor. His current research interests include intelligent control, networked control systems, signal processing, and autonomous driving.

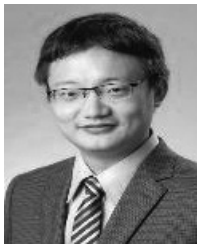

Ming Liu received the B.A. degree in automation from Tongji University, Shanghai, China, in 2005, and the Ph.D. degree in robotics from the Department of Mechanical Engineering and Process Engineering, ETH Zürich, Zürich, Switzerland, in 2013.

He was a Visiting Scholar with Erlangen Nurnberg University, Erlangen, Germany, and the Fraunhofer Institute IISB, Erlangen. He is currently an Assistant Professor with the Department of Electronic and Computer Engineering, Hong Kong University of Science and Technology, Hong Kong. His current research interests include autonomous mapping, visual navigation, topological mapping, and environment modeling.

Qijun Chen (SM'16) received the B.S. degree in automatic control from the Huazhong University of Science and Technology, Wuhan, China, in 1987, the M.S. degree in control engineering from Xi'an Jiaotong University, Xi'an China, in 1990, and the Ph.D. degree in control theory and control engineering from Tongji University, Shanghai, China, in 1999.

He was a Visiting Professor with the University of California at Berkeley, Berkeley, CA, USA, in 2008. He is currently a Professor with the College of Electronic and Information Engineering, Tongji University. His current research interest includes network-based control systems and robotics.